Synthesis of $(\mu\text{-H})_3Ru_3(\mu_3\text{-CSEt})(CO)_9$ and Its Rearrangement to $(\mu\text{-H})Ru_3(\mu_3\text{-}\eta^2\text{-}CH_2SEt)(CO)_9$. Crystal Structure of $(\mu\text{-H})Ru_3(\mu_3\text{-}\eta^2\text{-}CH_2SEt)(CO)_9$[1]

Melvyn Rowen Churchill,* Joseph W. Ziller, Dennis M. Dalton, and Jerome B. Keister*

Department of Chemistry, University at Buffalo, State University of New York, Buffalo, New York 14214

Received October 6, 1986

$(\mu\text{-H})_3Ru_3(\mu_3\text{-CSEt})(CO)_9$ is synthesized by treatment of $(\mu\text{-H})_3Ru_3(\mu_3\text{-CBr})(CO)_9$ with ethanethiol and triethylamine and has been fully characterized by spectroscopic methods. Upon heating at 50–60 °C, $(\mu\text{-H})_3Ru_3(\mu_3\text{-CSEt})(CO)_9$ rearranges to $(\mu\text{-H})Ru_3(\mu_3\text{-}\eta^2\text{-}CH_2SEt)(CO)_9$ (46% yield), characterized by spectroscopy and by X-ray crystallography. $(\mu\text{-H})Ru_3(\mu_3\text{-}\eta^2\text{-}CH_2SEt)(CO)_9$ crystallizes in the centrosymmetric monoclinic space group $P2_1/n$ (No. 14) with a = 8.2639 (10) Å, b = 16.8680 (17) Å, c = 13.7886 (15) Å, β = 93.788 (9)°, V = 1917.9 (4) Å^3, and Z = 4. X-ray diffraction data (Mo Kα, 2θ = 4.5–45.0°) were collected with a Syntex $P2_1$ automated four-circle diffractometer, and the structure was refined to R_F = 6.0% for all 2523 unique reflections (R_F = 2.9% for those 1732 reflections with $|F_o| > 6\sigma(|F_o|)$). The complex contains a triangular cluster of ruthenium atoms, each of which is linked to three terminal carbonyl ligands. The $\mu_3\text{-}\eta^2\text{-}CH_2SEt$ ligand caps the triruthenium cluster with the sulfur atom bridging Ru(2) and Ru(3) [Ru(2)–S = 2.348 (2) Å, Ru(3)–S = 2.302 (2) Å, and Ru(2)–S–Ru(3) = 73.07 (7)°] and with the methylene carbon atom, C(1), bonded to Ru(1) [Ru(1)–C(1) = 2.188 (9) Å]. A hydride ligand bridges the Ru(1)–Ru(2) edge in the equatorial plane, with Ru(1)–H(12) = 1.61 (7), Ru(2)–H(12) = 1.87 (7) Å, and Ru(1)–H(12)–Ru(2) = 117 (4)°. The Ru–Ru bond distances are inequivalent [Ru(1)–Ru(2) = 2.974 (1), Ru(1)–Ru(3) = 2.818 (1), and Ru(2)–Ru(3) = 2.769 (1) Å], with the edge bridged by the hydride ligand having the longest distance. The rearrangement of $(\mu\text{-H})_3Ru_3(\mu_3\text{-CSEt})(CO)_9$ to $(\mu\text{-H})Ru_3(\mu_3\text{-}\eta^2\text{-}CH_2SEt)(CO)_9$ involves two C–H reductive eliminations, the two unsaturated metal atoms thus formed being stabilized by coordination of the sulfur atom. Thus, $(\mu\text{-H})Ru_3(\mu_3\text{-}\eta^2\text{-}CH_2SEt)(CO)_9$ is a stabilized alkyl analogous to an intermediate in the previously reported "desorption" of CH_3X from $(\mu\text{-H})_3Ru_3(\mu_3\text{-CX})(CO)_9$ (X = Ph, Cl, or CO_2Me) forming $Ru_3(CO)_{12}$ under a CO atmosphere.

The chemistry of the $(\mu\text{-H})_3Ru_3(\mu_3\text{-CX})(CO)_9$ cluster series has proved to be a important entry into a basic understanding of fundamental processes occurring on polymetallic units. The mechanisms of ligand substitution,[1a] reductive elimination of molecular hydrogen,[2] hydrogen transfer to unsaturated hydrocarbons,[3] and insertion of alkynes into the Ru–C bond[4] have been investigated in our laboratory. The structures,[5] bonding,[6] and spectroscopic properties[7] of these clusters have also been the subjects of recent studies. The nature of the methylidyne substituent frequently has a major role in determining the chemistry of the cluster. For example, in reactions of $(\mu\text{-H})_3Ru_3(\mu_3\text{-CX})(CO)_9$ with CO, reductive elimination of hydrogen occurs when X is OMe[2] but reductive elimination of CH_3X proceeds when X is CO_2Me, Cl, Ph, and others.[8] To further investigate the influence of the substituent upon the reactivity of these clusters, we have prepared the new cluster $(\mu\text{-H})_3Ru_3(\mu_3\text{-CSEt})(CO)_9$ and report here its thermally induced rearrangement to $(\mu\text{-H})Ru_3(\mu_3\text{-}\eta^2\text{-}CH_2SEt)(CO)_9$, fully characterized by X-ray crystallography.[9] This rearrangement involves reductive elimination of two C–H bonds, the first two in the sequence leading to alkane from $(\mu\text{-H})_3Ru_3(\mu_3\text{-CX})(CO)_9$. Elsewhere we have reported that a single C–H reductive elimination occurs upon pyrolysis of $(\mu\text{-H})_3Ru_3(\mu_3\text{-CCO}_2Me)(CO)_9$, forming the stabilized alkylidene $(\mu\text{-H})_2Ru_3(\mu_3\text{-}\eta^2\text{-CHC(O)OMe})(CO)_9$, also characterized by X-ray crystallography.[1f]

Experimental Section

General Data. $(\mu\text{-H})_3Ru_3(\mu_3\text{-CBr})(CO)_9$ was prepared by a previously published procedure.[10] Infrared spectra were recorded on a Beckman 4250 spectrophotometer as cyclohexane solutions and were referenced to the 2138.5 cm^{-1} absorption due to cyclohexane. ^1H and ^{13}C NMR spectra were recorded on a JEOL FX-90Q spectrometer; $Cr(acac)_3$ (0.02 M) was added as a relaxation agent for the ^{13}C spectra. Mass spectra were recorded at the Penn State University Mass Spectrometry Center by Dr. R. Minard. Elemental analyses were obtained from Schwarzkopf Microanalytical Laboratories.

$(\mu\text{-H})_3Ru_3(\mu_3\text{-CSEt})(CO)_9$. Ethanethiol (46 μL, 0.63 mmol) and triethylamine (52 μL, 0.38 mmol) were added to a solution of $(\mu\text{-H})_3Ru_3(\mu_3\text{-CBr})(CO)_9$ (81.6 mg, 0.125 mmol) in 5 mL of dry cyclohexane. The mixture was stirred under nitrogen at room

(1) This paper constitutes part 13 of the series "Structural Studies on Ruthenium Carbonyl Hydrides". Recent previous parts include the following. (a) Part 7: Abdul Rahman, Z.; Beanan, L. R.; Bavaro, L. M.; Modi, S. P.; Keister, J. B.; Churchill, M. R. *J. Organomet. Chem.* **1984**, *263*, 75. (b) Part 8: Churchill, M. R.; Fettinger, J. C.; Keister, J. B. *Organometallics* **1985**, *4*, 1867. (c) Part 9: Churchill, M. R.; Fettinger, J. C.; Keister, J. B.; See, R. F.; Ziller, J. W. *Organometallics* **1985**, *4*, 2112. (d) Part 10: Churchill, M. R.; Ziller, J. W.; Keister, J. B. *J. Organomet. Chem.* **1985**, *297*, 93. (e) Part 11: Churchill, M. R.; Duggan, T. P.; Keister, J. B.; Ziller, J. W. *Acta Crystallogr., Sect. C: Cryst. Struct. Commun.*, accepted for publication. (f) Part 12: Churchill, M. R.; Janik, T. S.; Duggan, T. P.; Keister, J. B. *Organometallics*, preceding paper in this issue.

(2) (a) Bavaro, L. M.; Montangero, P.; Keister, J. B. *J. Am. Chem. Soc.* **1983**, *105*, 4977. (b) Bavaro, L. M.; Keister, J. B. *J. Organomet. Chem.* **1985**, *287*, 357. (c) Dalton, D. M.; Barnett, D. J.; Duggan, T. P.; Keister, J. B.; Malik, P. T.; Modi, S. P.; Shaffer, M. R.; Smesko, S. A. *Organometallics* **1985**, *4*, 1854.

(3) Churchill, M. R.; Beanan, L. R.; Wasserman, H. J.; Bueno, C.; Abdul Rahman, Z.; Keister, J. B. *Organometallics* **1983**, *2*, 1179.

(4) Beanan, L. R.; Keister, J. B. *Organometallics* **1985**, *4*, 1713.

(5) (a) Zhu, N. J.; Lecomte, C.; Coppens, P.; Keister, J. B. *Acta Crystallogr., Sect. B: Struct. Crystallogr. Cryst. Chem.* **1982**, *B38*, 1286. (b) Sheldrick, G. M.; Yesinowski, J. P. *J. Chem. Soc., Dalton Trans.* **1975**, 873. (d) Castiglioni, M.; Gervasio, G.; Sappa, E. *Inorg. Chim. Acta* **1981**, *49*, 217.

(6) Sherwood, D. E., Jr.; Hall, M. B. *Organometallics* **1982**, *1*, 1519.

(7) (a) Oxton, I. A. *Spectrochim. Acta, Part A* **1982**, *38A*, 181. (b) Evans, J.; McNulty, G. S. *J. Chem. Soc., Dalton Trans.* **1984**, 79.

(8) Duggan, T. P.; Barnett, D. J.; Muscatella, M. J.; Keister, J. B. *J. Am. Chem. Soc.* **1986**, *108*, 6076.

(9) A preliminary report of the syntheses and spectroscopic characterizations has appeared: Dalton, D. M.; Keister, J. B. *J. Organomet. Chem.* **1985**, *290*, C37.

(10) Keister, J. B.; Horling, T. L. *Inorg. Chem.* **1980**, *19*, 2304.

0276-7333/87/2306-0806$01.50/0

Table I. Experimental Data for the X-ray Diffraction Study of $(\mu\text{-H})Ru_3(\mu_3\text{-}\eta^2\text{-}CH_2SEt)(CO)_9$

(A) Crystallographic Parameters at 20 °C (293 K)

cryst system: monoclinic	formula: $C_{12}H_8O_9Ru_3S$
space group: $P2_1/n$ (No. 14)	mol wt 631.5
a = 8.2639 (10) Å	Z = 4
b = 16.8680 (17) Å	D(calcd) = 2.19 g cm^{-3}
c = 13.7886 (15) Å	μ(Mo Kα) = 24.2 cm^{-1}
β = 93.788 (9)°	
V = 1917.9 (4) Å^3	

(B) Collection of X-ray Diffraction Data

diffractometer: Syntex $P2_1$
radiation: Mo K$\bar{\alpha}$ ($\bar{\lambda}$ = 0.710 730 Å)
monochromator: highly oriented (pyrolytic) graphite, 2θ(m) = 12.160° for 002 reflection, equatorial mode, assumed to be 50% perfect/50% ideally mosaic for polarization correction
reflctions measd: $+h,+k,\pm l$ for 2θ = 4.5–45.0°; 2726 reflections measured and merged to 2523 unique data; no datum rejected
scan type: coupled θ(crystal)–2θ(counter)
scan width: [2θ(Mo Kα_1) – 0.9] → [2θ(Mo Kα_2) + 0.9]°
scan speed: 4.0 deg min^{-1}
background measurement: stationary crystal and stationary counter at each end of the 2θ scan; each for one-half of total scan time

temperature for 8 h. Evaporation of the solvent and purification by preparative TLC (silica gel, cyclohexane/dichloromethane, 5:1) yielded $(\mu\text{-H})_3Ru_3(\mu_3\text{-CSEt})(CO)_9$ as an orange powder (40.2 mg, 0.064 mmol, 51%). In a typical reaction, the 5:3:1 molar ratio of HSEt:Et_3N:$(\mu\text{-H})_3Ru_3(\mu_3\text{-CBr})(CO)_9$ resulted in yields ranging from 40 to 60%. Increased reaction times caused excessive decomposition of the cluster as did use of dichloromethane as the solvent. $(\mu\text{-H})_3Ru_3(\mu_3\text{-CSEt})(CO)_9$ was crystallized from methanol as dark orange crystals.

Anal. Calcd for $C_{12}H_8O_9Ru_3S$: C, 22.82; H, 1.28. Found: C, 22.82; H, 1.57. IR (C_6H_{12}): ν(CO) 2107 vw, 2080 vs, 2036 vs, 2029 m, 2019 s, 2007 vw cm^{-1}. ^{1}H NMR ($CDCl_3$, 25 °C): 3.18 (q, 2 H, CH_2), 1.40 (t, 3 H, CH_3), –17.55 (s, 3 H, RuHRu) ppm. $^{13}C\{^1H\}$ NMR ($CDCl_3$, 22 °C): 204.4 (1 C, methylidyne carbon), 189.5 (3 C, axial CO), 189.4 (6 C, equatorial CO), 43.3 (1 C, SCH_2Me), 12.9 (1 C, CH_3) ppm. EI MS: m/z 634 ($^{102}Ru_3$).

$(\mu\text{-H})Ru_3(\mu_3\text{-}\eta^2\text{-}CH_2SEt)(CO)_9$. $(\mu\text{-H})_3Ru_3(\mu_3\text{-CSEt})(CO)_9$ (110 mg, 0.174 mmol) was dissolved in 20 mL of dry cyclohexane under nitrogen. The mixture was heated at 55–60 °C for 51 h, resulting in a dark orange-brown solution. Following evaporation of the solvent, the residue was dissolved in dichloromethane and purified by preparative TLC (silica gel, cyclohexane/dichloromethane, 5:1) yielding crude orange-yellow crystals of $(\mu\text{-H})Ru_3(\mu_3\text{-}\eta^2\text{-}CH_2SEt)(CO)_9$ (51 mg, 0.081 mmol, 46%). Recrystallization from methanol provided well-formed yellow crystals suitable for X-ray analysis.

Anal. Calcd for $C_{12}H_8O_9Ru_3S$: C, 22.82; H, 1.28. Found: C, 22.85; H, 1.14. IR (C_6H_{12}): ν(CO) 2089 m, 2060 s, 2036 vs, 2017 s, 2005 m, 2000 m cm^{-1}. ^{1}H NMR ($CDCl_3$, 22 °C): 2.47 (q, 2 H_a, $-SCH_2Me$), 1.37 (d, 2 H_b, $-CH_2SEt$), 1.13 (t, 3 H_c, CH_3), –16.58 (t, 1 H_d, RuHRu) ppm, J_{ac} = 7.3 Hz, J_{bd} = 1.5 Hz. $^{13}C\{^1H\}$ NMR ($CDCl_3$, 23 °C): 196.7 (1 C), 194.0 (br, 8 C), 54.5 (1 C, SCH_2Me), 11.4 (1 C, CH_3), –9.9 (1 C, CH_2SEt) ppm. EI MS: m/z 634 ($^{102}Ru_3$).

Collection of X-ray Diffraction Data for $(\mu\text{-H})Ru_3(\mu_3\text{-}\eta^2\text{-}CH_2SEt)(CO)_9$. A yellow crystal of approximate dimensions 0.10 × 0.13 × 0.20 mm^3 was sealed in a glass capillary under a nitrogen atmosphere and accurately aligned on our Syntex $P2_1$ automated diffractometer. Subsequent set-up operations (determination of accurate cell dimensions and orientation matrix) and collection of the intensity data were carried out by the previously described techniques of this laboratory;[11] details appear in Table I. The systematic absences $h0l$ for $h + l = 2n + 1$ and $0k0$ for $k = 2n + 1$ uniquely define the centrosymmetric monoclinic space group $P2_1/n$.

All data were corrected for the effects of absorption (μ = 24.2 cm^{-1}) and for Lorentz and polarization effects, were converted to unscaled $|F_o|$ values, and were placed on an approximate absolute scale by means of a Wilson plot. Any reflection with I(net) < 0 was assigned the value $|F_o| = 0$. No datum was rejected.

(11) Churchill, M. R.; Lashewycz, R. A.; Rotella, F. J. *Inorg. Chem.* **1977**, *16*, 265.

Table II. Final Positional Parameters for $(\mu\text{-H})Ru_3(\mu_3\text{-}\eta^2\text{-}CH_2SEt)(CO)_9$

atom	x	y	z	B_{iso}, Å^2
Ru(1)	0.187 30 (8)	0.378 94 (4)	0.140 59 (5)	
Ru(2)	0.258 02 (8)	0.384 76 (4)	0.354 78 (5)	
Ru(3)	0.484 29 (8)	0.433 75 (4)	0.228 01 (5)	
S	0.425 84 (26)	0.304 27 (12)	0.265 34 (16)	
C(1)	0.310 7 (12)	0.265 53 (48)	0.167 51 (68)	
C(2)	0.571 5 (15)	0.232 87 (68)	0.320 87 (84)	
C(3)	0.689 1 (15)	0.206 13 (82)	0.247 60 (87)	
O(11)	0.337 44 (85)	0.386 73 (37)	–0.054 60 (48)	
O(12)	0.030 95 (94)	0.542 75 (41)	0.119 92 (55)	
O(13)	–0.102 82 (85)	0.282 32 (44)	0.057 83 (55)	
O(21)	0.497 0 (10)	0.402 29 (45)	0.530 78 (55)	
O(22)	0.012 6 (11)	0.282 54 (51)	0.455 71 (59)	
O(23)	0.118 08 (85)	0.549 87 (42)	0.383 29 (56)	
O(31)	0.676 60 (82)	0.429 64 (40)	0.047 02 (53)	
O(32)	0.772 53 (92)	0.467 58 (55)	0.371 53 (65)	
O(33)	0.380 45 (89)	0.605 83 (37)	0.209 54 (56)	
C(11)	0.282 5 (10)	0.385 32 (46)	0.020 38 (66)	
C(12)	0.089 8 (11)	0.482 55 (56)	0.128 19 (63)	
C(13)	–0.001 5 (11)	0.318 81 (53)	0.092 43 (66)	
C(21)	0.408 4 (12)	0.396 77 (52)	0.464 31 (72)	
C(22)	0.103 6 (12)	0.319 92 (59)	0.419 71 (69)	
C(23)	0.169 0 (11)	0.488 33 (58)	0.372 97 (64)	
C(31)	0.602 5 (11)	0.430 69 (50)	0.114 45 (73)	
C(32)	0.663 0 (12)	0.454 41 (63)	0.317 46 (80)	
C(33)	0.421 2 (11)	0.541 19 (55)	0.216 52 (65)	
H(12)	0.115 0 (88)	0.369 5 (37)	0.245 7 (53)	4.8 (18)
H(1A)	0.402 (12)	0.242 4 (58)	0.103 3 (76)	9.9 (30)
H(1B)	0.231 5 (91)	0.224 7 (45)	0.187 3 (55)	4.9 (20)
H(2A)	0.514 (10)	0.185 3 (55)	0.344 7 (65)	6.4 (24)
H(2B)	0.635 (11)	0.269 1 (55)	0.368 7 (70)	7.3 (29)
H(3A)	0.755 9	0.164 7	0.271 0	6.0
H(3B)	0.737 0	0.244 9	0.216 4	6.0
H(3C)	0.615 1	0.176 6	0.192 2	6.0

Solution and Refinement of the Structure. All calculations were performed on our locally modified version of the Syntex XTL system. The analytical form of the appropriate neutral atom scattering factor was corrected for both the real ($\Delta f'$) and imaginary ($i\Delta f''$) components of anomalous dispersion.[12] The function minimized during least-squares refinement was $\sum w(|F_o| - |F_c|)^2$, where $w = [(\sigma|F_o|)^2 + (0.015|F_o|)^2]^{-1}$.

The structure was solved by using direct methods (MULTAN).[13] The positions of the three ruthenium atoms were determined from an E map. All remaining atoms (other than the hydrogen atoms of the methyl group centered on C(3)) were located from a series of difference Fourier syntheses. Hydrogen atoms of the methyl group were included in calculated positions with d(C–H) = 0.95 Å[14] and were included in a staggered conformation. Refinement of positional and anisotropic thermal parameters for all non-hydrogen atoms and positional and isotropic parameters for the hydride ligand and hydrogen atoms of the methylene groups led to convergence with[15] R_F = 6.0%, R_{wF} = 3.9%, and GOF = 1.17 for 246 variables refined against all 2523 reflections. (Data/parameter ratio = 10.3:1.) Residuals for those 2019 reflections with $|F_o| > 3\sigma(|F_o|)$ were R_F = 3.9%, R_{wF} = 3.5% and for those 1732 reflections with $|F_o| > 6\sigma(|F_o|)$ were R_F = 2.9% and R_{wF} = 3.0%. An isotropic correction for secondary extinction was applied.

Analysis of the function $\sum w(|F_o| - |F_c|)^2$ showed no unusual trends as a function of Miller indices, magnitude of $|F_o|$, $(\sin\theta)/\lambda$, or sequence number. A final difference Fourier synthesis was essentially featureless. The structure is thus both correct and

(12) *International Tables for X-Ray Crystallography*; Kynoch: Birmingham, England, 1974; Vol. 4: (a) pp 99–101; (b) pp 149–150.
(13) Germain, G.; Main, P.; Woolfson, M. M. *Acta Crystallogr., Sect. A: Cryst. Phys., Diffr., Theor. Gen. Crystallogr.* **1971**, *A27*, 368.
(14) Churchill, M. R. *Inorg. Chem.* **1973**, *12*, 1213.
(15) R_F (%) = $100\sum||F_o| - |F_c||/\sum|F_o|$; R_{wF} (%) = $100[\sum w(|F_o| - |F_c|)^2/\sum w|F_o|^2]^{1/2}$; GOF = $[\sum w(|F_o| - |F_c|)^2/(NO - NV)]^{1/2}$, with NO = number of observations and NV = number of variables

complete. Final atomic positions are collected in Table II. Anisotropic thermal parameters appear as supplementary material.

Results

Synthesis of $(\mu\text{-H})_3Ru_3(\mu_3\text{-CSEt})(CO)_9$. Our synthesis of $(\mu\text{-H})_3Ru_3(\mu_3\text{-CSEt})(CO)_9$ was developed by analogy to the base-catalyzed displacement of halide used to prepare $(\mu\text{-H})_3Ru_3(\mu_3\text{-COEt})(CO)_9$[10] and $Co_3(\mu_3\text{-CSR})(CO)_9$.[16] Best yields were obtained from reactions of $(\mu\text{-H})_3Ru_3(\mu_3\text{-CBr})(CO)_9$ with 5 equiv of ethanethiol and 3 equiv of triethylamine in cyclohexane solution and by allowing the reaction to proceed only until the IR spectrum indicated that no starting material remained. No reaction under these conditions occurred in the absence of triethylamine. Poorer yields were obtained in more polar solvents such as dichloromethane, acetonitrile, or THF. With a large excess of ethanethiol extensive decomposition resulted. Low yields were also obtained by using NaSEt/ethanethiol (0–10%), LiSEt/ethanethiol (0–10%), $NaHCO_3$/ethanethiol (0–10%), ethanethiol/dichloromethane (10%), $Me_2Sn(SEt)_2$/dichloromethane (0–5%),[26] or ethanethiol alone (0–10%).

The new cluster $(\mu\text{-H})_3Ru_3(\mu_3\text{-CSEt})(CO)_9$ is a red-orange crystalline solid, air-stable and soluble in common organic solvents. The EI mass spectrum displays the molecular ion and ions resulting from stepwise loss of the CO ligands; satisfactory elemental analyses were obtained. The IR spectrum contains absorptions due to terminal CO stretching modes in a rather simple pattern characteristic of molecules of this class.[7,10] The ^1H NMR spectrum consists of a singlet at −17.55 ppm due to three equivalent bridging hydride ligands and resonances due to the Et group (3.18 (2 H, q) and 1.40 (3 H, t) ppm, J = 7.2 Hz). The ^{13}C NMR spectrum consists of a resonances at 204.4 (1 C) ppm, assigned to the methylidyne carbon, 189.5 (3 C) ppm, assigned to the axial carbonyls, 189.4 (6 C) ppm, assigned to the equatorial carbonyls, 43.3 (1 C) ppm, assigned to the methylene carbon, and 12.9 (1 C) ppm, assigned to the methyl carbon.

Synthesis of $(\mu\text{-H})Ru_3(\mu_3\text{-}\eta^2\text{-}CH_2SEt)(CO)_9$. The nature of the methylidyne substituent X is an important factor that determines the path of the reaction of $(\mu\text{-H})_3Ru_3(\mu_3\text{-CX})(CO)_9$ with CO. We had previously noted that strong π-donating substituents, such as OMe or NMe_2, facilitate reductive elimination of hydrogen, forming $(\mu\text{-H})Ru_3(\mu\text{-CX})(CO)_{10}$,[2] whereas for other substituents, such as Ph, Cl, or CO_2Me, the most facile pathway is reductive elimination of CH_3X.[8] Since the SEt group should be a poorer π-donor than OMe but a better one than Ph or Cl, both reaction paths were possibilities. Unexpectedly, $(\mu\text{-H})_3Ru_3(\mu_3\text{-CSEt})(CO)_9$, even in the presence of CO (1 atm), rearranges to $(\mu\text{-H})Ru_3(\mu_3\text{-}\eta^2\text{-}CH_2SEt)(CO)_9$ (Figure 1), characterized by spectroscopic methods and by X-ray crystallography.

At 70.6 °C the rate constant for the rearrangement of $(\mu\text{-H})_3Ru_3(\mu_3\text{-CSEt})(CO)_9$ to $(\mu\text{-H})Ru_3(\mu_3\text{-}\eta^2\text{-}CH_2SEt)(CO)_9$ in decahydronaphthalene solution and under a nitrogen atmosphere is 2.2×10^{-4} s^{-1}, corresponding to a free energy of activation of 25.9 kcal/mol. However, the rate is dependent upon the solvent, apparently increasing with increasing solvent polarity. At 25 °C in acetone solution the rearrangement is ca. 50% complete after 60 h. A complete kinetic study of the reaction is in progress, and the results will be published in a later paper.

$(\mu\text{-H})Ru_3(\mu_3\text{-}\eta^2\text{-}CH_2SEt)(CO)_9$ is a yellow crystalline solid that is soluble in common organic solvents. Although the

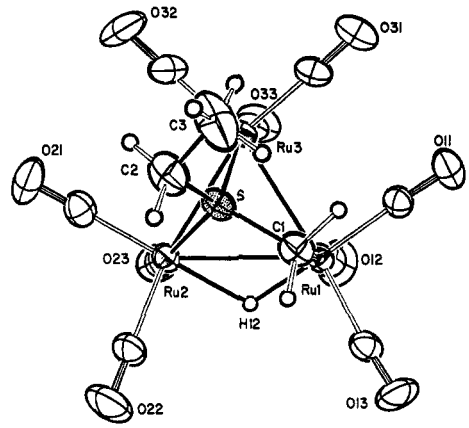

Figure 1. Labeling of atoms in the $(\mu\text{-H})Ru_3(\mu_3\text{-}\eta^2\text{-}CH_2SEt)(CO)_9$ molecule [ORTEP-II diagram; 30% probability ellipsoids for all non-hydrogen atoms; hydrogen atoms artificially reduced].

composition of the product was readily apparent from the spectroscopic data, the connectivity, particularly of the SEt and methylene groups, could not be established without recourse to X-ray crystallography. The EI mass spectrum is very similar to that of $(\mu\text{-H})_3Ru_3(\mu_3\text{-CSEt})(CO)_9$, displaying the molecular ion and ions derived by sequential loss of CO. The IR spectrum contains only terminal CO stretches. The ^1H NMR spectrum at room temperature consists of resonances at −16.58 (t, 1 H, RuHRu) and 1.37 (d, 2 H, CH_2SEt) ppm coupled to one another with a coupling constant of 1.5 Hz, in addition to resonances due to the SEt group (2.47 (q, 2 H, SCH_2Me) and 1.13 (t, 3 H, CH_3) ppm, J = 7.3 Hz). Although the protons of both methylene groups are diastereotopic, only single resonances are seen for each set at room temperature.

Both ^1H and ^{13}C NMR spectra show evidence for fluxional processes. At −60 °C the static proton spectrum displays nonequivalent methylene reasonances for the SEt group; although the other methylene protons are also diastereotopic, there is apparently an insignificant difference between the chemical shifts of these two since only a broad singlet is observed. An estimate of the free energy of activation, 51 (± 2) kJ/mol (12.2 (± 0.5) kcal/mol), was determined from the apparent coalescence temperature of −35 °C for the two quartets of the SEt protons.[17] A mechanism that would account for the observed spectra is exchange of the hydride between the two Ru–Ru edges not bridged by S; this would generate an apparent plane of symmetry bisecting the methylene protons. Such fluxional processes are commonly observed for $(\mu\text{-H})_2M_3(\mu_3\text{-}\eta^2\text{-L})(CO)_9$ clusters.[18] Indeed, we have reported a closely related exchange process for $(\mu\text{-H})_2Ru_3(\mu_3\text{-}\eta^2\text{-}CHC(O)OCH_3)(CO)_9$ having $\Delta G^\ddagger < 54$ kJ/mol (13 kcal/mol).

The ^{13}C NMR spectrum at 23 °C also exhibits fluxional behavior. Only two signals, a sharp peak at 196.7 ppm and a very broad one at 194.0 ppm with relative areas of 1:8, appear in the carbonyl region; we did not attempt to obtain the static spectrum. We presume that the sharp signal is due to the unique CO ligand trans to the alkyl carbon. Some process or processes involving CO migration, in addition to hydride migration, are required to average the other eight resonances. The CH_2SEt resonance occurs at

(16) Seyferth, D.; Rudie, C. N.; Merola, J. S. *J. Organomet. Chem.* **1978**, *144*, C26.

(17) At −59 °C the separation between the two quartets is 6.8 Hz. Our best estimate of the coalescence temperature is −35 °C. At coalescence: $k_c = 2^{1/2}\pi\Delta\nu$, where $\Delta\nu$ is the separation in hertz in the absence of exchange: Wilkins, R. G. *The Study of Kinetics and Mechanism of Reactions of Transition Metal Complexes*; Allyn and Bacon: Boston, 1974; p 154.

(18) For examples see ref 1f and other references therein.

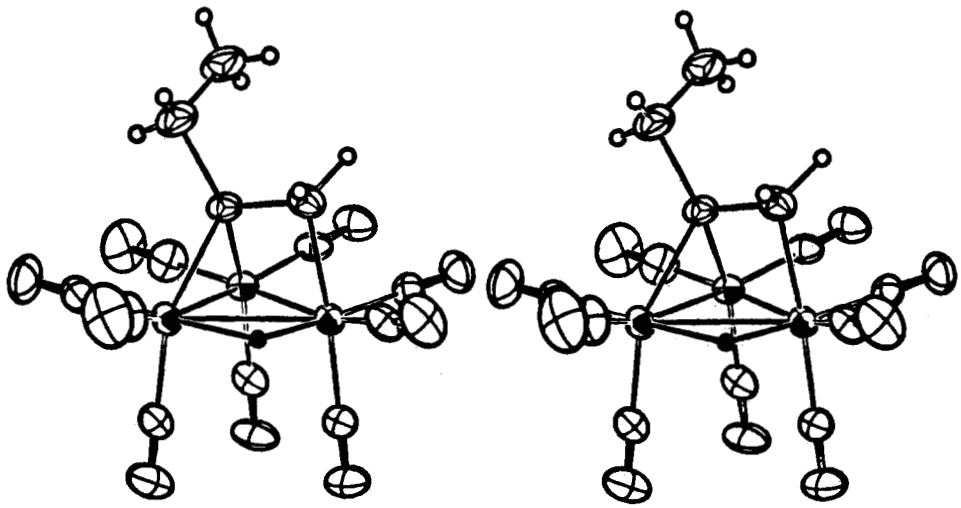

Figure 2. Stereoscopic view of the $(\mu\text{-}H)Ru_3(\mu_3\text{-}\eta^2\text{-}CH_2SEt)(CO)_9$ molecule.

Table III. Interatomic Distances (Å) for $(\mu\text{-}H)Ru_3(\mu_3\text{-}\eta^2\text{-}CH_2SEt)(CO)_9$

(A) Ru–Ru, Ru–CH_2SEt, and Ru–(μ-H) Distances			
Ru(1)–Ru(2)	2.974 (1)	Ru(2)–S	2.348 (2)
Ru(1)–Ru(3)	2.818 (1)	Ru(3)–S	2.302 (2)
Ru(2)–Ru(3)	2.769 (1)	Ru(1)–C(1)	2.188 (9)
Ru(1)–H(12)	1.61 (7)	Ru(2)–H(12)	1.87 (7)
(B) Ru–CO and C–O Distances			
Ru(1)–C(11)	1.884 (9)	C(11)–O(11)	1.157 (11)
Ru(1)–C(12)	1.927 (9)	C(12)–O(12)	1.129 (12)
Ru(1)–C(13)	1.941 (9)	C(13)–O(13)	1.120 (12)
Ru(2)–C(21)	1.902 (10)	C(21)–O(21)	1.138 (13)
Ru(2)–C(22)	1.944 (10)	C(22)–O(22)	1.122 (13)
Ru(2)–C(23)	1.918 (10)	C(23)–O(23)	1.133 (12)
Ru(3)–C(31)	1.900 (10)	C(31)–O(31)	1.147 (12)
Ru(3)–C(32)	1.893 (10)	C(32)–O(32)	1.156 (13)
Ru(3)–C(33)	1.890 (9)	C(33)–O(33)	1.143 (11)
(C) S–C and C–C Distances within the CH_2SEt Ligand			
S–C(1)	1.727 (10)	C(2)–C(3)	1.516 (17)
S–C(2)	1.834 (12)		

Table IV. Interatomic Angles (deg) for $(\mu\text{-}H)Ru_3(\mu_3\text{-}\eta^2\text{-}CH_2SEt)(CO)_9$

(A) Angles within the $Ru_3(\mu_3\text{-}\eta^2\text{-}CH_2SEt)$ System			
Ru(3)–Ru(1)–Ru(2)	57.04 (2)	Ru(2)–Ru(1)–C(1)	78.55 (24)
Ru(1)–Ru(2)–Ru(3)	58.64 (2)	Ru(3)–Ru(1)–C(1)	80.28 (24)
Ru(2)–Ru(3)–Ru(1)	64.32 (2)	Ru(2)–S–C(1)	108.36 (32)
Ru(2)–S–Ru(3)	73.07 (7)	Ru(3)–S–C(1)	107.29 (32)
Ru(1)–Ru(2)–S	62.84 (5)	Ru(1)–C(1)–S	91.62 (40)
Ru(3)–Ru(2)–S	52.70 (5)		
Ru(1)–Ru(3)–S	66.10 (6)		
Ru(2)–Ru(3)–S	54.22 (6)		
(B) Ru–Ru–CO Angles			
Ru(2)–Ru(1)–C(11)	143.7 (3)	Ru(3)–Ru(1)–C(11)	87.4 (3)
Ru(2)–Ru(1)–C(12)	96.4 (3)	Ru(3)–Ru(1)–C(12)	95.0 (3)
Ru(2)–Ru(1)–C(13)	117.2 (3)	Ru(3)–Ru(1)–C(13)	167.3 (3)
Ru(1)–Ru(2)–C(21)	150.1 (3)	Ru(1)–Ru(3)–C(31)	96.8 (3)
Ru(1)–Ru(2)–C(22)	110.3 (3)	Ru(1)–Ru(3)–C(32)	163.6 (3)
Ru(1)–Ru(2)–C(23)	96.2 (3)	Ru(1)–Ru(3)–C(33)	92.9 (3)
Ru(3)–Ru(2)–C(21)	92.1 (3)	Ru(2)–Ru(3)–C(31)	156.6 (3)
Ru(3)–Ru(2)–C(22)	161.8 (3)	Ru(2)–Ru(3)–C(32)	100.0 (3)
Ru(3)–Ru(2)–C(23)	95.2 (3)	Ru(2)–Ru(3)–C(33)	98.3 (3)
(C) OC–Ru–CO and Ru–C–O Angles			
C(11)–Ru(1)–C(12)	93.8 (4)	Ru(1)–C(11)–O(11)	177.4 (8)
C(11)–Ru(1)–C(13)	95.9 (4)	Ru(1)–C(12)–O(12)	178.9 (8)
C(12)–Ru(1)–C(13)	97.0 (4)	Ru(1)–C(13)–O(13)	173.8 (8)
C(21)–Ru(2)–C(22)	96.2 (4)	Ru(2)–C(21)–O(21)	178.3 (9)
C(21)–Ru(2)–C(23)	92.0 (4)	Ru(2)–C(22)–O(22)	178.7 (9)
C(22)–Ru(2)–C(23)	100.6 (4)	Ru(2)–C(23)–O(23)	179.2 (8)
C(31)–Ru(3)–C(32)	96.9 (4)	Ru(3)–C(31)–O(31)	178.5 (8)
C(31)–Ru(3)–C(33)	96.4 (4)	Ru(3)–C(32)–O(32)	179.4 (9)
C(32)–Ru(3)–C(33)	94.4 (4)	Ru(3)–C(33)–O(33)	178.9 (8)
(D) OC–Ru–S and OC–Ru–C Angles			
C(21)–Ru(2)–S	95.8 (3)	C(33)–Ru(3)–S	150.2 (3)
C(22)–Ru(2)–S	110.2 (3)	C(11)–Ru(1)–C(1)	89.0 (4)
C(23)–Ru(2)–S	147.1 (3)	C(12)–Ru(1)–C(1)	174.4 (4)
C(31)–Ru(3)–S	106.6 (3)	C(13)–Ru(1)–C(1)	87.5 (4)
C(32)–Ru(3)–S	101.3 (3)		
(E) Angles Involving the $\mu_3\text{-}\eta^2\text{-}CH_2SEt$ and μ-H Ligands			
Ru(2)–S–C(2)	123.7 (4)	Ru(1)–Ru(2)–H(12)	28.8 (21)
Ru(3)–S–C(2)	125.1 (4)	Ru(2)–Ru(1)–H(12)	33.9 (25)
S–C(2)–C(3)	110.4 (8)	Ru(1)–H(12)–Ru(2)	117 (4)
Ru(3)–Ru(2)–H(12)	87.2 (21)	S–Ru(2)–H(12)	82.1 (21)
Ru(3)–Ru(1)–H(12)	90.7 (25)	C(1)–Ru(1)–H(12)	87.6 (25)
C(11)–Ru(1)–H(12)	176.3 (25)		
C(21)–Ru(2)–H(12)	177.8 (22)		

–9.9 ppm, 214 ppm upfield from the chemical shift of the methylidyne carbon resonance of $(\mu\text{-}H)_3Ru_3(\mu_3\text{-}CSEt)(CO)_9$. This is consistent with the general trend in ^{13}C chemical shifts: $M_3(\mu\text{-}CR) > M_2(\mu\text{-}CR_2) > MCR_3$.[19]

Description of the Crystal and Molecular Structure of $(\mu\text{-}H)Ru_3(\mu_3\text{-}\eta^2\text{-}CH_2SEt)(CO)_9$. The crystal contains discrete molecular units of $(\mu\text{-}H)Ru_3(\mu_3\text{-}\eta^2\text{-}CH_2SEt)(CO)_9$ that are separated by normal van der Waals' distances; there are no abnormally short intermolecular contacts. Each molecule is chiral, but the crystal contains an ordered racemic mixture by virtue of the inversion centers and n glide planes present in space group $P2_1/n$. The atomic labeling scheme and molecular geometry are illustrated in Figure 1. Figure 2 provides a stereoscopic view of the molecule. Interatomic distances and angles are collected in Tables III and IV.

The $(\mu\text{-}H)Ru_3(\mu_3\text{-}\eta^2\text{-}CH_2SEt)(CO)_9$ molecule is based upon a triangular array of ruthenium atoms. Each ruthenium atom is in a different stereochemical environment, and each is linked to three terminal carbonyl ligands (two equatorial and one axial). The $\mu_3\text{-}\eta^2\text{-}CH_2SEt$ ligand caps the triangular ruthenium cluster with the sulfur atom bridging Ru(2) and Ru(3) (Ru(2)–S = 2.348 (2) Å, Ru(3)–S = 2.302 (2) Å, and Ru(2)–S–Ru(3) = 73.07 (7)°) and with the methylene carbon atom, C(1), bonded to Ru(1) via Ru(1)–C(1) = 2.188 (9) Å. The three Ru–Ru linkages are inequivalent. That bridged by the μ-SEt ligand is the shortest, with Ru(2)–Ru(3) = 2.769 (1) Å; this is contracted relative to the μ-hydrido–μ-thioethyl-bridged Ru–Ru distance of 2.843 (1) Å in $(\mu\text{-}H)Ru_3(CO)_{10}(\mu\text{-}SEt)$.[1d] The Ru(1)–Ru(2) linkage is the longest; this equatorially hy-

(19) A pertinent example is the series $(\mu\text{-}H)_3Os_3(\mu_3\text{-}CH)(CO)_9$, $(\mu\text{-}H)_2Os_3(\mu\text{-}CH_2)(CO)_{10}$, and $(\mu\text{-}H)Os_3(\mu\text{-}\eta^2\text{-}CH_3)(CO)_{10}$, for which the ^{13}C chemical shifts are 118.4, 25.8, and –59.2 ppm, respectively.[32]

drido-bridged distance is expanded to 2.974 (1) Å, in agreement with the equatorially hydrido-bridged Ru–Ru bond length of 2.967 (1) Å in $(\mu\text{-H})_2Ru_3(\mu_3\text{-}\eta^2\text{-CHC(O)OCH}_3)(CO)_9$[1f] and with measurements from other equatorially hydrido-bridged M–M systems.[20-22] The nonbridged Ru(1)–Ru(3) distance is 2.818 (1) Å (cf. Ru–Ru(av) = 2.854 (5) Å in the parent binary carbonyl $Ru_3(CO)_{12}$[23]).

The trinuclear cluster is associated with a total of 48 outer valence electrons. (Using the neutral atom/neutral ligand electron-counting formalism, we get 24 electrons from the three d^8 Ru(0) atoms, 18 electrons from the nine terminal carbonyl ligands, 5 electrons from the $\mu_3\text{-}\eta^2\text{-CH}_2\text{SEt}$ ligand, and 1 electron from the μ-hydride ligand.) Electron counts at the individual metal centers are inequivalent with 18 electrons at Ru(3), $17^1/_2$ electrons at Ru(1), and $18^1/_2$ electrons at Ru(2).

If we ignore the direct Ru(1)-Ru(2) interaction,[24] then each ruthenium atom is seen to have an approximately octahedral coordination environment. The $Ru(CO)_3$ groups are associated with OC–Ru–CO angles of 92.0 (4)–100.6 (4)°, the μ-hydride ligand lies in a position trans to two carbonyl ligands (C(11)–Ru(1)–H(12) = 176.3 (25)° and C(21)–Ru(2)–H(12) = 177.8 (22)°), the methylene carbon is trans to a carbonyl group (C(1)–Ru(1)–C(12) = 177.4 (4)°), and the sulfur atom is in a distorted trans configuration relative to two other carbonyl ligands (C(23)–Ru(2)–S = 147.1 (3)° and C(33)–Ru(3)–S = 150.2 (3)°).

The μ-hydride ligand was located with limited precision (Ru(1)–H(12) = 1.61 (7) Å, Ru(2)–H(12) = 1.87 (7) Å, and Ru(1)–H(12)–Ru(2) = 117 (4)°) but appears to be close to coplanar with the triruthenium plane. (The deviation from the Ru_3 plane is −0.14 (6) Å, and the dihedral angle between Ru(1)–Ru(2)–Ru(3) and Ru(1)–H(12)–Ru(2) planes is 171.3°—see Table V.)

The $\mu_3\text{-}\eta^2\text{-CH}_2\text{SEt}$ ligand appears to incorporate a normal Ru–C σ bond (Ru(1)–C(1) = 2.188 (4) Å as compared to a predicted Ru–C distance of approximately 2.20 Å based upon $r(C(sp^3))$ = 0.77 Å and r(Ru) = 1.43 Å from $^1/_2$(Ru–Ru) in $Ru_3(CO)_{12}$). The sulfur atom has a distorted (chiral) tetrahedral environment in which the S–C(1) distance of 1.727 (10) Å is significantly shorter than the *normal* S–C(2) distance of 1.834 (12) Å (cf. the accepted C–S distance of 1.817 ± 0.005 Å in paraffinic and saturated heterocyclic thio compounds[25]).

The Ru–CO bond lengths range from 1.884 (9) through 1.944 (10) Å. Although there is little variation in these distances, the longest are trans to Ru–Ru bonds (Ru(2)–C(22) = 1.944 (10) and Ru(1)–C(13) = 1.941 (9) Å) and the shortest is trans to the μ-hydride ligand (Ru(1)–C(11) = 1.884 (9) Å). There is no clear difference between axial and equatorial Ru–CO distances.

Finally, we note that C–O distances range only from 1.120 (12) through 1.157 (11) Å and that all Ru–C–O systems are close to linear (173.8 (8)° → 179.4 (9)°).

Discussion

Halide Displacement from $(\mu\text{-H})_3Ru_3(\mu_3\text{-CBr})(CO)_9$. Few clusters containing the CSR ligand have previously been prepared. Reactions of $Co_3(\mu_3\text{-CBr})(CO)_9$ with arenethiols and triethylamine or with $Me_2Sn(SR)_2$ were used to prepare a number of examples of the type $Co_3(\mu_3\text{-CSR})(CO)_9$.[16,26] The mixed-metal analogue $Cp_2Fe_2Co(\mu_3\text{-CSMe})(CO)_7$ was synthesized via the reaction of $[Co(CO)_4^-]$ with $[Cp_2Fe_2(\mu\text{-CSMe})(\mu\text{-CO})(CO)_2^+]$, prepared by methylation of the corresponding thiocarbonyl.[27] It is worthy of note that the CSMe ligand of $Cp_2Fe_2Co(\mu_3\text{-CSMe})(CO)_7$ is bound through carbon to all three metals and also through sulfur to the cobalt. The most likely explanation for the ability of the CSR ligand to bond in an η^2 fashion is the strength of the M–S bond.

The synthesis of $(\mu\text{-H})_3Ru_3(\mu_3\text{-CSEt})(CO)_9$ was derived from earlier work by Seyferth and co-workers (in which base-catalyzed attack by thiols on $Co_3(\mu_3\text{-CBr})(CO)_9$ afforded the analogous $Co_3(\mu_3\text{-CSR})(CO)_9$ clusters)[16] and from our previous synthesis of $(\mu\text{-H})_3Ru_3(\mu_3\text{-COEt})(CO)_9$ by reaction of $(\mu\text{-H})_3Ru_3(\mu_3\text{-CBr})(CO)_9$ with sodium ethoxide/ethanol.[10] As noted by Seyferth, these reactions are unlikely to involve direct attack of the nucleophile on the alkylidyne carbon. Substitution of alkoxide for bromide in alcohol solution may involve an S_N1-type mechanism; removal of bromide with $AlCl_3$ in unreactive solvents forms $[(\mu\text{-H})_3Ru_3(\mu_3\text{-CCO})(CO)_9^+]$, and treatment of $(\mu\text{-H})_3Ru_3(\mu_3\text{-CBr})(CO)_9$ with $AlCl_3$/benzene generates $(\mu\text{-H})_3Ru_3(\mu_3\text{-CPh})(CO)_9$, both reactions presumably involving the intermediacy of $[H_3Ru_3(C)(CO)_9^+]$.[10] However, this is unlikely to be the case for replacement of bromide by thiolates in nonpolar solvents such as cyclohexane. Sey-

Table V. Important Molecular Planes and Atomic Deviations Therefrom (Å) for $(\mu\text{-H})Ru_3(\mu_3\text{-}\eta^2\text{-CH}_2\text{SEt})(CO)_9$

(A) The Triruthenium Plane

$0.3707X - 0.9286Y - 0.0181Z + 5.4443 = 0$[a]

Ru(1)*[b]	0.000	O(13)	0.673 (7)
Ru(2)*	0.000	C(21)	0.208 (9)
Ru(3)*	0.000	O(21)	0.354 (8)
S	1.827 (2)	C(22)	0.505 (10)
H(12)	−0.14 (6)	O(22)	0.790 (9)
C(1)	2.139 (8)	C(23)	−1.906 (10)
C(2)	3.359 (12)	O(23)	−3.032 (7)
C(3)	4.181 (14)	C(31)	0.477 (8)
C(11)	0.262 (8)	O(31)	0.760 (7)
O(11)	0.452 (6)	C(32)	0.171 (11)
C(12)	−1.914 (9)	O(32)	0.269 (9)
O(12)	−3.033 (7)	C(33)	−1.870 (9)
C(13)	0.392 (9)	O(33)	−3.003 (6)

(B) The Ru(2)–S–Ru(3) Plane

$0.6545X - 0.0228Y - 0.7557Z + 5.0209 = 0$[a]

Ru(2)*	0.000	C(1)	1.596 (10)
Ru(3)*	0.000	H(12)	1.85 (7)
S*	0.000	C(2)	−1.305 (12)
Ru(1)	2.484 (1)	C(3)	−1.212 (12)

(C) The Ru(2)–H(12)–Ru(1) Plane

$-0.2276X + 0.9738Y - 0.0023Z - 5.8967 = 0$[a]

Ru(1)*	0.000	C(1)	−2.090 (8)
Ru(2)*	0.000	S	−1.653 (2)
H(12)*	0.000	C(2)	−3.090 (12)
Ru(3)	0.357 (1)	C(3)	−3.763 (14)

(D) Dihedral Angles

plane A/B	101.99° (78.01°)
plane A/C	171.32° (8.68°)
plane B/C	82.62° (97.38°)

[a] Orthonormal coordinates. [b] Only atoms marked with an asterisk were used in calculating the plane.

(20) Churchill, M. R.; DeBoer, B. G.; Rotella, F. J. *Inorg. Chem.* **1976**, *15*, 1843.
(21) (a) Churchill, M. R.; DeBoer, B. G. *Inorg. Chem.* **1977**, *16*, 878. (b) Churchill, M. R.; DeBoer, B. G. *Inorg. Chem.* **1977**, *16*, 2397.
(22) (a) Churchill, M. R. *Adv. Chem. Ser.* **1978**, *No. 167*, 36. (b) Teller, R. G.; Bau, R. *Struct. Bonding (Berlin)* **1981**, *44*, 1.
(23) Churchill, M. R.; Hollander, F. J. Hutchinson, J. P. *Inorg. Chem.* **1977**, *16*, 2655.
(24) Kampe, C. E.; Boag, N. M.; Knobler, C. B.; Kaesz, H. D. *Inorg. Chem.* **1984**, *23*, 1390.
(25) *Spec. Publ.—Chem. Soc.* **1965**, *No. 18*, p S22s.
(26) Seyferth, D.; Merola, J. S.; Berry, D. H. *Z. Anorg. Allg. Chem.* **1979**, *458*, 267.
(27) Schroeder, N. C.; Richardson, J. W., Jr.; Wang, S.-L.; Jacobson, R. A.; Angelici, R. J. *Organometallics* **1985**, *4*, 1226.

ferth and co-workers have proposed a radical chain mechanism of the $S_{RN}1$ type. We believe that this mechanism, shown in Scheme I, is also appropriate for the ruthenium analogues. In support of this mechanism: (1) the yields are higher in nonpolar solvents, but the reaction does require the presence of triethylamine, (2) the yields are quite variable under apparently identical conditions, suggesting the presence of radical intermediates, and (3) treatment of $(\mu\text{-}H)_3Ru_3(\mu_3\text{-}CBr)(CO)_9$ with triethylamine/phenol in dichloromethane yields only $(\mu\text{-}H)_3Ru_3(\mu_3\text{-}CH)(CO)_9$, not $(\mu\text{-}H)_3Ru_3(\mu_3\text{-}COPh)(CO)_9$, suggesting the intermediacy of the $[H_3Ru_3(C)(CO)_9^{\bullet}]$ radical.[28] Further experiments designed to probe the mechanism of this reaction are in progress.

Scheme I

$$H_3Ru_3(CBr)(CO)_9 + SEt^- \rightarrow [H_3Ru_3(CBr)(CO)_9^{\bullet -}] + SEt^{\bullet}$$

$$[H_3Ru_3(CBr)(CO)_9^{\bullet -}] \rightarrow [H_3Ru_3(C)(CO)_9^{\bullet}] + Br^-$$

$$[H_3Ru_3(C)(CO)_9^{\bullet}] + SEt^- \rightarrow [H_3Ru_3(CSEt)(CO)_9^{\bullet -}]$$

$$H_3Ru_3(CSEt)(CO)_9^{\bullet -} + H_3Ru_3(CBr)(CO)_9 \rightarrow H_3Ru_3(CSEt)(CO)_9 + H_3Ru_3(CBr)(CO)_9^{\bullet -}$$

Reductive Elimination of CH_3X from Trimetallic Clusters. An Analogy to Metal Surface Chemistry? Relatively few alkyl-containing clusters have been prepared previously. Some examples include $HOs_3(CH_2CO_2Et)(CO)_{10}$,[29] $HOs_3(CHMeCO_2Et)(CO)_{10}$,[29] $HOs_3(CH(CO_2Et)CH_2CO_2Et)(CO)_{10}$,[29] $HOs_3(CHMeOMe)(CO)_{10}$,[30] $HOs_3(CHMeSPh)(CO)_{10}$,[31] $HOs_3(CH_3)(CO)_{10}$,[32] $HOs_3(CH_2CH_3)(CO)_{10}$,[33] $Os_3(CH_3)(I)(CO)_{10}$,[34] and $HOs_3(NCO)(\text{succinoyl})(CO)_{10}$.[35] Several examples are stabilized by coordination of a substituent group on the alkyl chain (in some cases an agostic hydrogen) that acts as a two-electron donor, but all containing hydride ligands are unstable with respect to reductive elimination and those with β-hydrogens unstable to alkene elimination in the presence of donor ligands. None of these have been formed by reductive elimination reactions. To our knowledge there are no previous reports of Ru analogues, although alkyl intermediates must be important in the formation of $Ru_3(X)(OCEt)(CO)_{10}$ (X = Cl, Br, or I) and $HRu_3(OCEt)(CO)_{10}$ from $HRu_3(X)(CO)_{10}$ and $HRu_3(CO)_{11}^-$, respectively,[36] and in alkene hydroformylation and hydrogenation catalyzed by Ru clusters.[3,37]

The rearrangement of $(\mu\text{-}H)_3Ru_3(\mu_3\text{-}CSEt)(CO)_9$ to $(\mu\text{-}H)Ru_3(\mu_3\text{-}\eta^2\text{-}CH_2SEt)(CO)_9$ involves the migration of two hydride ligands to the methylidyne carbon and coordination of the sulfur atom to the two unsaturated metal atoms thus formed. The strength of the Ru–S bonds makes possible the isolation of the alkyl-containing cluster even under an atmosphere of carbon monoxide. Cleavage of a single Ru–S bond and the addition of carbon monoxide presumably should form $HRu_3(\mu\text{-}\eta^2\text{-}CH_2SEt)(CO)_{10}$, analogous to $HOs_3(CHMeSPh)(CO)_{10}$.[31] Thermolysis of other clusters $(\mu\text{-}H)_3Ru_3(\mu_3\text{-}CX)(CO)_9$ (X = Ph, Cl, or CO_2Me) or of $(\mu\text{-}H)_2Ru_3(\mu_3\text{-}\eta^2\text{-}CHCO_2CH_3)(CO)_9$ under CO forms the appropriate alkane and $Ru_3(CO)_{12}$.[8]

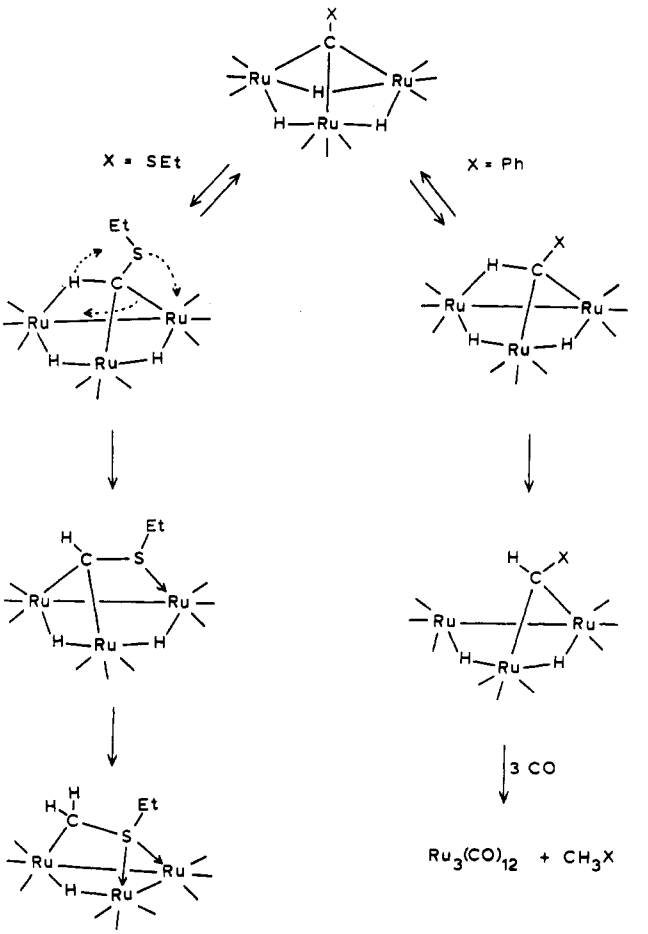

Figure 3. Proposed mechanism for isomerization of $(\mu\text{-}H)_3Ru_3(\mu_3\text{-}CSEt)(CO)_9$ to $(\mu\text{-}H)Ru_3(\mu_3\text{-}\eta^2\text{-}CH_2SEt)(CO)_9$.

The mechanism of rearrangement of $(\mu\text{-}H)_3Ru_3(\mu_3\text{-}CSEt)(CO)_9$ to $(\mu\text{-}H)Ru_3(\mu_3\text{-}\eta^2\text{-}CH_2SEt)(CO)_9$ is of interest with respect to the mechanism of cleavage of CH_3X from $(\mu\text{-}H)_3Ru_3(\mu_3\text{-}CX)(CO)_9$ (X = Ph, Cl, or CO_2Me) under CO. We have proposed that the mechanism of reductive cleavage involves a preequilibrium between the ground state and a tautomer containing an agostic Ru–H–CX bond, with the rate-determining step being cleavage of the Ru–H–CX bond to form an unsaturated intermediate (Figure 3).[8] It may be significant that the free energies of activation for rearrangement of $(\mu\text{-}H)_3Ru_3(\mu_3\text{-}CCO_2Me)(CO)_9$ to $(\mu\text{-}H)_2Ru_3(\mu_3\text{-}\eta^2\text{-}CHCO_2CH_3)(CO)_9$ ($\Delta G^{\ddagger}$ = 112 kJ/mol (26.7 kcal/mol) at 70 °C)[1f] and for rearrangement of $(\mu\text{-}H)_3Ru_3(\mu_3\text{-}CSEt)(CO)_9$ to $(\mu\text{-}H)Ru_3(\mu_3\text{-}\eta^2\text{-}CH_2SEt)(CO)_9$ ($\Delta G^{\ddagger}$ = 108 kJ/mol (25.9 kcal/mol) at 70 °C), both reactions forming products in which the methylidyne substituent ends up coordinated to the cluster, are much lower than the free energies of activation for reductive elimination of CH_3X from $(\mu\text{-}H)_3Ru_3(\mu_3\text{-}CX)(CO)_9$ (X = Ph or Cl; $\Delta G^{\ddagger}$ = 129 and 123 kJ/mol, respectively) where X cannot act as a ligand.[8] This suggests that when X has Lewis base character, it may participate directly in the reductive elimination process by stabilization of the incipient site of unsaturation (Figure 3).

(28) Bower, D. K.; Keister, J. B., unpublished results.
(29) Keister, J. B.; Shapley, J. R. *J. Am. Chem. Soc.* **1976**, *98*, 1056.
(30) Boyar, E.; Deeming, A. J.; Arce, A. J.; De Sanctis, Y. *J. Organomet. Chem.* **1984**, *276*, C45.
(31) Boyar, E.; Deeming, A. J.; Henrick, K.; McPartlin, M.; Scott, A. *J. Chem. Soc., Dalton Trans.* **1986**, 1431.
(32) Calvert, R. B.; Shapley, J. R. *J. Am. Chem. Soc.* **1977**, *99*, 5225; **1978**, *100*, 6544.
(33) Cree-Uchiyama, M.; Shapley, J. R.; St. George, G. M. *J. Am. Chem. Soc.* **1986**, *108*, 1316.
(34) Morrison, E. D.; Bassner, S. L.; Geoffroy, G. L. *Organometallics* **1986**, *5*, 408.
(35) Zuffa, J. L.; Gladfelter, W. L. *J. Am. Chem. Soc.* **1986**, *108*, 4669.
(36) Kampe, C. E.; Boag, N. M.; Kaesz, H. D. *J. Am. Chem. Soc.* **1983**, *105*, 2896.
(37) For representative examples, see: (a) Suss-Fink, G. *J. Organomet. Chem.* **1980**, *193*, C20. (b) Braca, G.; Sbrana, G. *Chim. Ind. (Milan)* **1974**, *56*, 110. (c) Zuffa, J. L.; Blohm, M. L.; Gladfelter, W. L. *J. Am. Chem. Soc.* **1986**, *108*, 552. (d) Doi, Y.; Koshizuka, K.; Keii, T. *Inorg. Chem.* **1982**, *21*, 2732. (e) Suss-Fink, G.; Herrmann, G. *J. Chem. Soc., Chem. Commun.* **1985**, 735.

The dependence of the rate of rearrangement upon the solvent is consistent with the existence of a preequilibrium involving an agostic Ru–H–CSEt bond. Solvent effects upon equilibria between observable analogues have been previously noted. For example, the equilibrium constant for eq 1 is solvent-dependent, increasing in the order benzene < dichloromethane < acetone.[32] Recently solvent effects upon equilibria in eq 2 and 3 have been reported.[38]

$$HOs_3(HCH_2)(CO)_{10} \rightleftharpoons H_2Os_3(CH_2)(CO)_{10} \quad (1)$$

$$H_3Fe_3(CH)(CO)_9 \rightleftharpoons H_2Fe_3(HCH)(CO)_9 \quad (2)$$

$$H_2Fe_3(HCH)(CO)_9 \rightleftharpoons HFe_3(H_2CH)(CO)_9 \quad (3)$$

Our observation that a single hydride migration occurs upon pyrolysis of $(\mu\text{-H})_3Ru_3(\mu_3\text{-}CCO_2Me)(CO)_9$, forming $(\mu\text{-H})_2Ru_3(\mu_3\text{-}\eta^2\text{-}CHCO_2CH_3)(CO)_9$,[1f] suggests that the two hydride migrations required to form $(\mu\text{-H})Ru_3(\mu_3\text{-}\eta^2\text{-}CH_2SEt)(CO)_9$ occur sequentially through the intermediacy of $(\mu\text{-H})_2Ru_3(\mu_3\text{-}\eta^2\text{-}CHSEt)(CO)_9$ that should have a structure analogous to that of $(\mu\text{-H})_2Ru_3(\mu_3\text{-}\eta^2\text{-}CHCO_2CH_3)(CO)_9$. Since we see no evidence for an intermediate in the formation of $(\mu\text{-H})Ru_3(\mu_3\text{-}\eta^2\text{-}CH_2SEt)(CO)_9$, this suggests that the second reductive elimination is faster than the first.

Increasing rates for successive C–H eliminations are suggested by other evidence as well. We have previously noted that for $(\mu\text{-H})_3Ru_3(\mu_3\text{-CX})(CO)_9$ the Ru–CX bond length increases in the order X = Cl < Me < *p*-tolyl, the same as the trend of decreasing H–CH_2X bond strength, and have thus proposed that the Ru–CX bond strength parallels that of the corresponding H–CH_2X bond. A structural comparison of $(\mu\text{-H})_3Ru_3(\mu_3\text{-CX})(CO)_9$ (X = Cl,[5a] Me,[5b] or *p*-tolyl[1e]), $(\mu\text{-H})_2Ru_3(\mu_3\text{-}\eta^2\text{-}CHCO_2CH_3)(CO)_9$,[1f] and $(\mu\text{-H})Ru_3(\mu_3\text{-}\eta^2\text{-}CH_2SEt)(CO)_9$ shows that there is an increase in the Ru–C bond length upon successive C–H eliminations. Thus, the average Ru–C bond length increases from $(\mu\text{-H})_3Ru_3(\mu_3\text{-CX})(CO)_9$ (average = 2.088 Å) to $(\mu\text{-H})_2Ru_3(\mu_3\text{-}\eta^2\text{-}CHCO_2CH_3)(CO)_9$ (average = 2.140 Å) to $(\mu\text{-H})Ru_3(\mu_3\text{-}\eta^2\text{-}CH_2SEt)(CO)_9$ (2.188 Å). This suggests that the Ru–C bond strength may decrease in the order Ru–μ_3-CX > Ru–μ_2-CHX > Ru–CH_2X. Another indication of the increasing facility of successive reductive eliminations is the qualitative order of increasing ease of decomposition of an analogous Os cluster series under CO: $(\mu\text{-H})_3Os_3(\mu_3\text{-CH})(CO)_9$ < $(\mu\text{-H})_2Os_3(\mu_2\text{-}CH_2)(CO)_{10}$ < $(\mu\text{-H})Os_3(\mu_2\text{-}\eta^2\text{-}CH_3)(CO)_{10}$.[32]

The increasing rates for successive C–H eliminations from clusters may have a parallel in metal surface chemistry. Some controversy exists concerning the rate-determining step in the reaction of CO with hydrogen to form methane (Scheme II). Sequential hydrogenation of surface carbide is the proposed mechanism. On the basis of inverse isotope effects for methanation on alumina- and silica-supported Ru, the rate-determining step was proposed to be one of the steps in which a C–H bond is formed,[39] and the inverse isotope effect for methanation on Ni was interpreted to indicate partial CO hydrogenation prior to C–O bond dissociation.[40] On the other hand, a SIMS study of methanation on Ni(111) identified surface-bound methylidyne, methylene, and methyl intermediates, all having similar (within an order of magnitude) surface concentrations,[41] and the rate of desorption of methane by combination of methyl and hydrogen atoms on the Ni(111) surface has been determined to be 10^6 times faster than the rate of CO hydrogenation,[42] thus indicating rate-determining C–O bond cleavage. However, the relative rates of the successive C–H bond-forming steps have not been determined.

Scheme II

$$CO \rightarrow C(ads) + O(ads)$$

$$C(ads) + H(ads) \rightarrow CH(ads)$$

$$CH(ads) + H(ads) \rightarrow CH_2(ads)$$

$$CH_2(ads) + H(ads) \rightarrow CH_3(ads)$$

$$CH_3(ads) + H(ads) \rightarrow CH_4(g)$$

These trimetallic cluster models may provide information concerning the structures of the surface-bound intermediates, the mechanism of the desorption process, and the relative rates of the individual steps. Investigations of the mechanisms of reductive elimination from these clusters are in progress.

Acknowledgment. This work was supported by the National Science Foundation through Grant CHE85-20276 to J. B. K.

Registry No. $(\mu\text{-H})_3Ru_3(\mu_3\text{-CBr})(CO)_9$, 73746-95-9; $(\mu\text{-H})_3Ru_3(\mu_3\text{-CSEt})(CO)_9$, 100852-22-0; $(\mu\text{-H})Ru_3(\mu_3\text{-}\eta^2\text{-}CH_2SEt)(CO)_9$, 100852-23-1; ethanethiol, 75-08-1.

Supplementary Material Available: A table of anisotropic thermal parameters (1 page); a listing of observed and calculated structure factor amplitudes (13 pages). Ordering information is given on any current masthead page.

(38) Dutta, T. K.; Vites, J.; Lynam, M. M.; Chipman, D. M.; Barreto, R. D.; Jacobsen, G. B.; Fehlner, T. P., in press.

(39) (a) Kellner, C. S.; Bell, A. T. *J. Catal.* **1981**, *67*, 175. (b) Kobori, Y.; Naito, S.; Onishi, T.; Tamaru, K. *J. Chem. Soc., Chem. Commun.* **1981**, 92.

(40) Mori, T.; Masuda, H.; Imai, H.; Miyamoto, A.; Baba, S.; Murakami, Y. *Chem. Lett.* **1981**, 831.

(41) Kaminsky, M. P.; Winograd, N.; Geoffroy, G. L. *J. Am. Chem. Soc.* **1986**, *108*, 1315.

(42) Yates, J. T., Jr.; Gates, S. M.; Russell, J. N., Jr. *Surf. Sci.* **1985**, *164*, L839.